A Methodology for Internal Light Sources Estimation

by S. Stephany, F. M. Ramos, H. F. de Campos Velho, and C. D. Mobley

ABSTRACT—A reconstruction technique of bioluminescence sources in natural waters from in situ irradiance data is presented. The inverse problem is formulated as a nonlinear constrained optimization problem, assuming that the bioluminescence unknown profile can be represented by a sum of distributed Gaussian sources. The objective function is defined as the square Euclidean norm of the difference vector between experimental and computed data. The authors use the Hydrolight 3.0 code, which solves numerically the time-independent one-dimensional radiative transfer equation in natural water bodies using the invariant imbedding theory. The proposed inversion technique was tested with noise-corrupted synthetic data and yielded good numerical results. The influence of the number of Gaussian sources, as well as their standard deviations in the estimation, is analyzed.

KEY WORDS—Inverse problem, bioluminescence sources, invariant imbedding method, radiative transfer equation

1. Introduction

Bioluminescence is the phenomenon of light emission by marine organisms, which range in size from bacteria to fish and are found everywhere in marine waters. Estimation of underwater bioluminescence sources is an inverse problem of great relevance in oceanography, particularly for the study of the biological-optical processes in the oceans (Mobley, 1994). Some recent articles have studied this subject (Sanchez, Yi, and McCormick, 1992; Tao, McCormick, and Sanchez, 1994).

The classical direct or forward radiative transfer problem in hydrologic optics involves the determination of the radiance distribution in a body of water given known boundary conditions and inherent optical properties. The corresponding inverse radiative transfer problem arises when physical properties and/or internal light sources must be estimated from radiometric measurements of underwater light fields. In the last decades, the development of inversion methodologies for radiative transfer problems has been an important research topic in many branches of science and engineering (McCormick, 1992).

In this paper, we present an implicit inversion technique for reconstruction of bioluminescent isotropic source distributions from in situ radiometric measurements. The algorithm is formulated as a constrained nonlinear optimization problem in which the direct problem is iteratively solved for successive approximations of the unknown parameters. Iteration proceeds until an objective function, representing a least squares fit of model results and experimental data, converges to a specified small value. We use the Hydrolight 3.0 code (Mobley, 1995), which solves numerically the time-independent one-dimensional radiative transfer equation in natural water bodies using the invariant imbedding theory.

This approach could be extended for fluorescence estimation, since it is possible to model this phenomenon as an internal source of light in the wavelength of fluorescence emission. Fluorescence is directly related to the concentration of chlorophyll (e.g., from phytoplankton) or pollutants, which have economical relevance.

2. Direct Model

Implicit inversion techniques require repeated resolution of the direct model. Various numerical models are used for computing underwater radiance distributions, generally involving Monte Carlo techniques (Mobley, Gentili, Gordon, and colleagues, 1993).

In the present study, the time-independent one-dimensional radiative transfer equation is solved by the Hydrolight 3.0 code using the invariant imbedding method described in Mobley (1989, 1994). This software computes spectral radiances and the upward/downward plane and scalar irradiances at chosen depths (equally spaced or not). The model inputs are the inherent optical properties of the water, the internal light sources, the sky spectral radiance distribution, the state of the wind-blown water surface, and the bottom boundary conditions.

The monochromatic radiance transfer equation, in terms of the optical depth ζ (with $d\zeta = c(z)\,dz$, where z is the vertical coordinate), is given by

$$\mu \frac{dL(\zeta,\xi)}{d\zeta} = -L(\zeta,\xi) + \omega_0(\zeta) \int_{\Xi} L(\zeta,\xi') \cdot \beta(\xi' \to \xi)\, d\xi' + S(\zeta,\xi) \ , \tag{1}$$

where L is the radiance; β is the scattering phase function; $\omega_0 = b/c$ is the single scattering albedo; $c = a + b$ is the beam attenuation coefficient; a and b are the absorption and scattering coefficients, respectively; $\xi'(\theta', \phi')$ and $\xi(\theta, \phi)$ are the incident and scattered directions, respectively, for an infinitesimal beam; θ is the polar angle; ϕ is the azimuthal angle; S is the source term; β is the scattering phase function; and $\mu = \cos(\theta)$.

Equation (1) can be directionally discretized by quad averaging in the unit sphere Ξ the radiances $L(\zeta; \theta, \phi)$ for a finite number of azimuthal and polar angles:

S. Stephany, F. M. Ramos, and H. F. de Campos Velho, Laboratório Associado de Computação e Matemática Aplicada (LAC), Instituto Nacional de Pesquisas Espaciais (INPE), São José dos Campos (SP), – BRASIL. C. D. Mobley, Sequoia Scientific, Inc., Mercer Island, WA 98040, USA.

Communicated by S. N. Atluri, 06/20/98.

$$\mu \frac{dL(\zeta;\theta_i,\phi_j)}{d\zeta} = -L(\zeta;\theta_i,\phi_j) + \omega_0(\zeta)\sum_r\sum_s L(\zeta;\theta_r,\phi_s) \cdot \beta(\theta_r,\phi_s \to \theta_i,\phi_j) + S(\zeta,\theta_i,\phi_j) \quad (2)$$

where

$$L(\zeta;\theta_i,\phi_j) = \frac{1}{\Xi_{ij}} \int_\theta \int_\phi L(\zeta;\theta,\phi)\,\sin\theta\, d\theta d\phi \quad . \quad (3)$$

The radiance can be spectrally decomposed using its Fourier polynomial representation. For convenience, downward radiances are denoted by "+" and upward radiances by "−":

$$\boldsymbol{L}^{\pm}(\zeta;\theta_i,\phi_j) = \sum_{l=0}^{n} \left[\boldsymbol{L}_1^{\pm}(\zeta;\theta_i,l)\,\cos(l\,\phi_j) + \boldsymbol{L}_2^{\pm}(\zeta;\theta_i,l)\,\sin(l\,\phi_j)\right] .$$

Then, the radiance can be expressed as two sets of vectors ($p = 1$ for the cosine spectral amplitude, and $p = 2$ for the sine spectral amplitude). For a given set, each l corresponds to a discretized azimuthal angle, and, for a given l, each column corresponds to a discretized polar angle:

$$\boldsymbol{L}_p^{\mp}(\zeta,l) = \left[L_p^{\mp}(\zeta;\theta_1,l) \quad L_p^{\mp}(\zeta;\theta_2,l) \quad L_p^{\mp}(\zeta;\theta_3,l) \quad \ldots \quad L_p^{\mp}(\zeta;\theta_m,l)\right].$$

Rewriting the radiative transfer equation, some terms can be identified as being the local spectral reflectance (ρ) and local spectral transmittance (τ) matrices, which lead to the local interaction equations that show how the light interacts locally with an infinite slab of water:

$$\mp\frac{d\,\boldsymbol{L}_p^{\mp}(\zeta,l)}{d\zeta} = \boldsymbol{L}_p^{\mp}(\zeta,l)\,\tau(\zeta,l) + \boldsymbol{L}_p^{\pm}(\zeta,l)\,\rho(\zeta,l) + S_p^{\mp}(\zeta,l) .$$

Grouping the upward/downward radiances as two-row matrices yields an even more compact form for the local interaction equations:

$$\frac{d\,\boldsymbol{L}_p(\zeta,l)}{d\zeta} = \boldsymbol{L}_p(\zeta,l)\,\boldsymbol{K}(\zeta,l) + \boldsymbol{S}_p,$$

where $\boldsymbol{L}_p = \left[\boldsymbol{L}_p^- \;\; \boldsymbol{L}_p^+\right]$; $\boldsymbol{S}_p = \left[S_p^- \;\; S_p^+\right]$; and $\boldsymbol{K}$ is the spectral local transfer matrix, which is an inherent optical property:

$$\boldsymbol{K}(\zeta,l) \equiv \begin{bmatrix} -\tau(\zeta,l) & \rho(\zeta,l) \\ -\rho(\zeta,l) & \tau(\zeta,l) \end{bmatrix}.$$

Concerning this equation, the fundamental solution $\boldsymbol{M}$, source free, must comply to the following matrix differential equation:

$$\frac{d\,\boldsymbol{M}(\zeta,l)}{d\zeta} = \boldsymbol{M}(w,\zeta;l)\;\boldsymbol{K}(\zeta;l)\;; \qquad \boldsymbol{M}(w,w;l) = \boldsymbol{I}_{m\times m},$$

where m is the dimension of the polar discretization.

This fundamental solution maps the radiances from one depth (level w, at the surface) to another (level ζ). For the nonhomogeneous case, there is an internal source term given by the convolution of the internal source with $\boldsymbol{M}$:

$$\boldsymbol{L}_p(\zeta;l) = \boldsymbol{L}_p(w;l)\;\boldsymbol{M}(w,\zeta;l) + \int_w^\zeta \boldsymbol{S}_p(\zeta';l)\;\boldsymbol{M}(\zeta',\zeta;l)\;d\zeta' .$$

The rearrangement of the expression leads to the spectral global interaction equations for a finite slab of water, as shown below (the $\boldsymbol{M}$ elements were rewritten as new matrices), where the $\boldsymbol{T}$s are called the spectral standard transmittance matrices and the $\boldsymbol{R}$s are called the spectral standard reflectance matrices that rule how the light is transported through the slab of water. This first set is for a slab between the surface (w) and a level ζ:

$$\begin{bmatrix} \boldsymbol{L}_p^-(w;l) \\ \boldsymbol{L}_p^+(\zeta;l) \end{bmatrix}^T = \begin{bmatrix} \boldsymbol{L}_p^-(\zeta;l) \\ \boldsymbol{L}_p^+(w;l) \end{bmatrix}^T \begin{bmatrix} \boldsymbol{T}_p^-(\zeta,w;l) & \boldsymbol{R}_p^+(\zeta,w;l) \\ \boldsymbol{R}_p^-(w,\zeta;l) & \boldsymbol{T}_p^+(w,\zeta;l) \end{bmatrix}.$$

A second set can be found for a slab between level ζ and the bottom (b):

$$\begin{bmatrix} \boldsymbol{L}_p^-(\zeta;l) \\ \boldsymbol{L}_p^+(b;l) \end{bmatrix}^T = \begin{bmatrix} \boldsymbol{L}_p^-(b;l) \\ \boldsymbol{L}_p^+(\zeta;l) \end{bmatrix}^T \begin{bmatrix} \boldsymbol{T}_p^-(b,\zeta;l) & \boldsymbol{R}_p^+(b,\zeta;l) \\ \boldsymbol{R}_p^-(\zeta,b;l) & \boldsymbol{T}_p^+(\zeta,b;l) \end{bmatrix}.$$

For both sets, the output (left-hand side) radiance amplitudes are unknown and the incident (right-hand side) radiance amplitudes are given. To solve the radiative transfer equation, the unknown spectral standard operators must be found (for clarity, the internal source term is not shown).

Instead of integrating the local interaction equations in order to find $\boldsymbol{M}$, a set of Riccati differential equations can be derived for these standard operators. This is achieved by differentiating the global interaction equations and using the former local interaction equations to replace the ζ derivatives of the amplitude radiances. Grouping terms in a convenient way and assuming that each equation must be equal to zero for any radiance amplitude leads to a set of Riccati differential equations for the spectral standard operators.

Integration of these equations for a "bare" slab of water yields these operators using formerly calculated local transmittances and reflections. Instead of solving the problem directly, the invariant imbedding method allows one to construct the water body by integrating the Riccati equations, imbedding adjacent layers of water. Boundary conditions are then imbedded into the bare-slab operators, completing the solution.

3. Inverse Problem

Inverse problems are mathematically ill posed in the sense that existence, uniqueness, or stability of their solutions cannot be ensured. Several methods have been proposed for solving inverse radiative transfer problems. An excellent overview of the recent developments is found in McCormick (1992). In this paper, we describe an implicit inversion technique for reconstruction of bioluminescent isotropic source distributions from in situ radiometric measurements.

The bioluminescence source term is approximated by a summation of isotropic Gaussian sources, with uniform standard deviation σ, as follows:

$$S(z,\theta,\phi) = S(z) = \sum_{k=1}^{N_p} \frac{p_k}{\sigma\sqrt{2\pi}}\, e^{-(z-z_k)^2/2\sigma^2}. \qquad (4)$$

Denoting by $\boldsymbol{p} = [\, p_1, p_2, \ldots, p_{N_p} \,]$ the vector of unknown bioluminescence Gaussian source strengths to be determined by the inverse analysis, the inverse radiative transfer problem can be formulated as a nonlinear constrained minimization problem,

$$\min J(\boldsymbol{p}) \;\; , \;\; l_q \le p_q \le u_q \;\; , \;\; q = 1, \ldots, N_p \;\; , \qquad (5)$$

where the lower and upper bounds l_q and u_q are chosen in order to allow the inversion to lie within some a priori known physical limits. The bioluminescent sources are equally spaced in depth, defining a source grid of resolution $\Delta z_p = z_{max}/N_p$, where z_{max} corresponds to maximum depth of the computational domain. The misfit between direct model and experimental data is given by

$$\begin{aligned} J(\boldsymbol{p}) \;=\; \sum_{i=1}^{N_z} \;& [\; (E^{\exp}_{u,i} - E_{u,i}(\boldsymbol{p}))^2 \\ & + (E^{\exp}_{d,i} - E_{d,i}(\boldsymbol{p}))^2 \\ + \;& (E^{\exp}_{0u,i} - E_{0u,i}(\boldsymbol{p}))^2 \\ & + (E^{\exp}_{0d,i} - E_{0d,i}(\boldsymbol{p}))^2 \;] \;. \end{aligned} \qquad (6)$$

The irradiance data are composed by the spectral upward and downward scalar irradiances, defined as $E_{0_{u/d}}(\zeta) = \int_{\Xi_{u/d}} L(\zeta,\xi)\, d\Omega$, and by the spectral upward and downward plane irradiances, defined as $E_{u/d}(\zeta) = \int_{\Xi_{u/d}} L(\zeta,\xi)\, \cos\theta\, d\Omega$, where $d\Omega = \sin\theta\, d\theta d\phi$ is an infinitesimal solid angle. These irradiances are given for $i = 1, 2, \ldots, N_z$ depths, defining an irradiance grid of resolution $\Delta z_E = z_{max}/N_z$.

In the absence of an explicit solution, the optimization problem defined by equation (5) is iteratively solved by the quasi-Newtonian optimization algorithm E04UCF from the NAG Fortran Library (1993). This approach has been previously adopted with success by Lesnic, Elliot, and Ingham (1995) and Ramos and de Campos Velho (1996). An outline of the algorithm is described below.

3.1 Optimization Algorithm

The minimization of the objective function $J(\boldsymbol{p})$ given by equation (5), subject to simple bounds on $\mathbf{p}$, is solved using a first-order optimization algorithm from the NAG Fortran Library (1993). This routine is designed to minimize an arbitrary smooth function subject to constraints (simple bounds, linear and nonlinear constraints), using a sequential programming method. For the nth iteration, the calculation proceeds as follows:

1. Solve the direct problem for $\boldsymbol{p}^n$ and compute the objective function $J(\boldsymbol{p}^n)$.
2. Compute by finite differences the gradient $\nabla J(\boldsymbol{p}^n)$.
3. Compute a positive-definite quasi-Newtonian approximation to the Hessian $\mathbf{H}^n$:

$$\mathbf{H}^n = \mathbf{H}^{n-1} + \frac{\mathbf{b}^n\,(\mathbf{b}^n)^T}{(\mathbf{b}^n)^T\,\mathbf{u}^n} - \frac{\mathbf{H}^{n-1}\,\mathbf{u}^n\,(\mathbf{u}^n)^T\,\mathbf{H}^{n-1}}{(\mathbf{u}^n)^T\,\mathbf{H}^{n-1}\,\mathbf{u}^n} \;\; ,$$

   where $\mathbf{b}^n = \boldsymbol{p}^n - \boldsymbol{p}^{n-1}$
   $\mathbf{u}^n = \nabla J(\boldsymbol{p}^n) - \nabla J(\boldsymbol{p}^{n-1})$.
4. Compute the search direction $\mathbf{d}^n$ as a solution of the following quadratic programming subproblem:

   Minimize $[\nabla J(\mathbf{p}^n)^n]^T\,\mathbf{d}^n + \frac{1}{2}(\mathbf{d}^n)^T\,(\mathbf{H}^n)\,\mathbf{d}^n$ subject to $l_q - p_q^n \le d_q \le u_q - p_q^n$.
5. Set $\boldsymbol{p}^{n+1} = \boldsymbol{p}^n + \beta^n\,\mathbf{d}^n$, where the step length β^n minimizes $J(\boldsymbol{p}^n + \beta^n\,\mathbf{d}^n)$.
6. Test the convergence; stop, or return to step 1.

4. Numerical Results

The performance of the inversion method presented in the previous section was evaluated for different values of the number of sources, N_p, and their standard deviation, σ. Synthetic irradiance data were generated by the same direct analytical model used in the inverse solver for a single wavelength $\lambda = 550$ nm. A 2% Gaussian noise was added to the exact values to reproduce actual experimental errors. The computational domain was discretized into a vertical irradiance grid of $N_z = 11$ nodes, ranging from 0 to 30 m. In all simulations, β was given by the one-term Henyey-Greenstein scattering phase function, defined as follows:

$$\beta(\psi) \;=\; \frac{1}{4\pi}(1-g^2)(1+g^2-2g\,\cos(\psi))^{-3/2} \;\; , \qquad (7)$$

where ψ is the scattering angle (formed by ξ' and ξ directions) and $g = 0.90$. The inherent optical properties were assumed to be constant, and Monterey Bay water conditions, under sunlight and without wind, were considered, taken from a similar work (Tao, McCormick, and Sanchez, 1994). At the sea surface, a cardioidal radiance distribution is taken to simulate the diffuse sunlight (1 W/m^2 nm), the bottom being considered an infinitely thick homogeneous layer of water.

The computations were performed until convergence was attained using a uniform zero-value bioluminescence profile as the starting point, $\boldsymbol{p}^0$. For each test case, we computed the normalized values of $J(\boldsymbol{p}^f)$ and the root mean square error, defined by

$$\epsilon = \left[\sum_{q=1}^{N_z} (p_q^f - p_q^{exact})^2 / (p_q^0 - p_q^{exact})^2 \right]^{1/2} \;\; , \qquad (8)$$

where p^f refers to the value of the vector of parameters after the final convergence of the inversion algorithm is attained.

4.1 Case 1

The inversion method was first applied to a bioluminescence profile consisting of two Gaussian sources located at depths of $z = 10.5$ m and 16.5 m, with $\sigma = 0.75$. Both the direct and inverse models were run for $N_z = 11$ and $N_p = 10$. This case was run without noise and 2% noise.

The evolution of the normalized objective function and root mean square error for the situations described above are plotted in Figures 1 and 2. It can be seen that there exists a delay between the objective function and the root mean square error decay. It is interesting to point out that, in the presence of noise, the objective function did not decay to zero. Numerical values for the normalized objective function and root mean square error are shown in Table 1. However, Figure 3 shows that the inversion algorithm properly recovered the source strength variation with z in both shape and magnitude.

4.2 Case 2

To check the proposed inversion technique in a more difficult configuration, we considered a bioluminescence profile generated by a combination of hyperbolic tangents, centered at a depth that does not match the source grid of the inverse model. In this second test case, due to the low resolution of the inversion grid, the exact solution was reconstructed by a set of neighboring sources, as presented in Figure 4. The accuracy of this result can be improved by increasing the number of sources N_p or by changing the standard deviation

TABLE 1—NOISE INFLUENCE FOR THE FINAL VALUES OF THE NORMALIZED OBJECTIVE FUNCTION AND ROOT MEAN SQUARE ERROR FOR TEST CASE 1

Noise	$J(\boldsymbol{p})/J(\boldsymbol{p}^0)$	ϵ
No noise	0.2241×10^{-9}	0.1689×10^{-4}
2% noise	$0.1889 \times 10^{+0}$	0.4692×10^{-1}

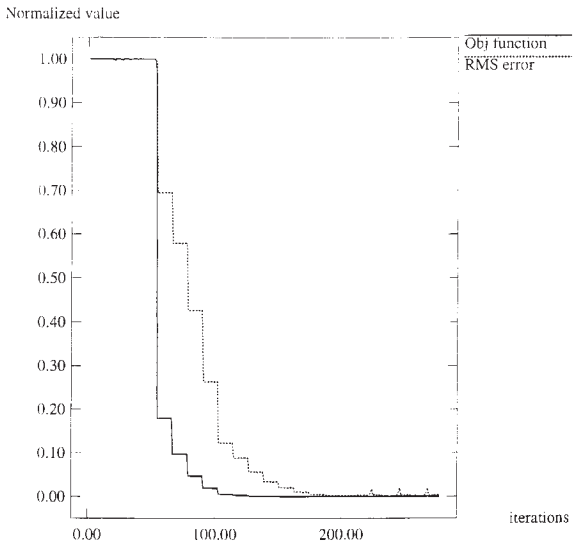

Figure 1. Normalized objective function and root mean square error for test case 1 (no noise, $\sigma = 0.75$, and $N_p = 10$).

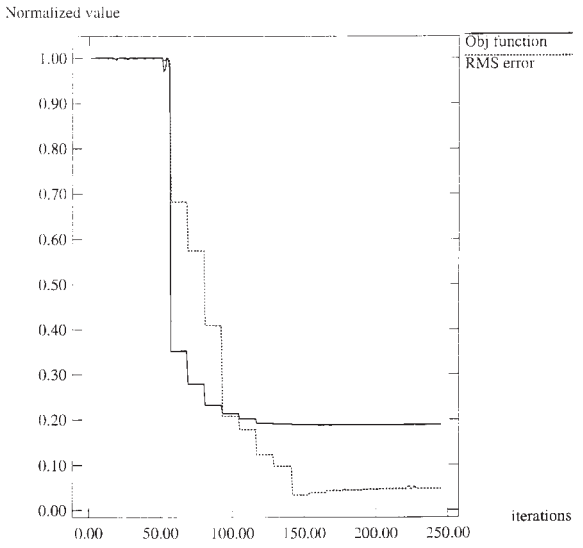

Figure 2. Normalized objective function and root mean square error for test case 1 (2% noise, $\sigma = 0.75$, and $N_p = 10$).

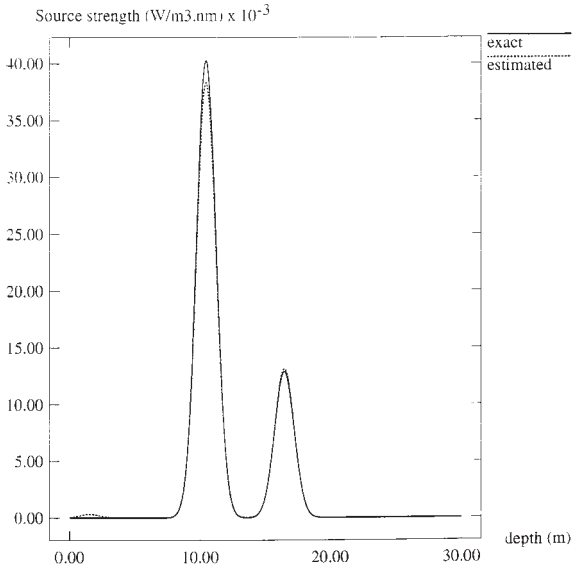

Figure 3. Estimated and exact profiles for test case 1 (2% noise, $N_p = 10$, $\sigma = 0.75$).

σ of the Gaussian sources in the inverse model, as shown in Figures 5 and 6 and Table 2. Obviously, the increase of N_p is more effective but demands more processing time.

5. Conclusion

In this paper, we introduced a reconstruction technique of bioluminescence sources in natural waters from in situ irradiance data. Assuming that the unknown bioluminescence profile can be represented by a sum of distributed Gaussian sources, the inverse problem was formulated as a nonlinear constrained optimization problem and iteratively solved by a quasi-Newtonian minimization routine.

The proposed inversion technique was tested with noise-corrupted synthetic data and yielded good numerical results. The influence of the number of Gaussian sources and their

TABLE 2—NORMALIZED OBJECTIVE FUNCTION AND ROOT MEAN SQUARE ERROR FOR TEST CASE 2

	$\sigma = 0.75$		$N_p = 10$	
	$N_p = 10$	$N_p = 20$	$\sigma = 0.75$	$\sigma = 1.50$
$J(\boldsymbol{p})/J(\boldsymbol{p}^0)$	0.319911	0.308089	0.319911	0.325750
ϵ	0.539159	0.180156	0.539159	0.229669

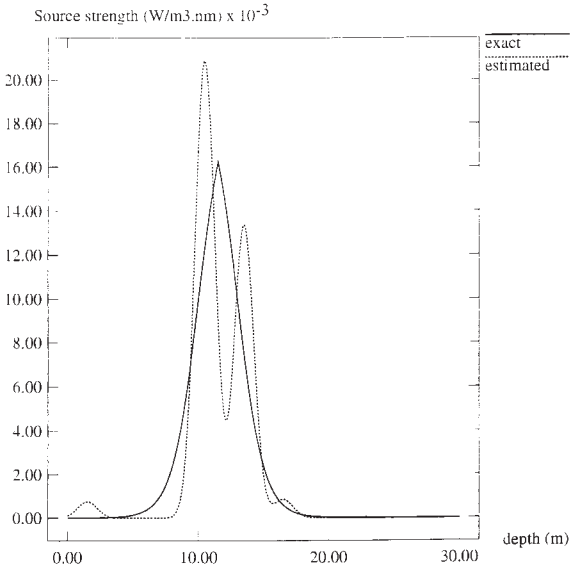

Figure 4. Estimated and exact profiles for test case 2 (2% noise, N_p = 10, σ = 0.75).

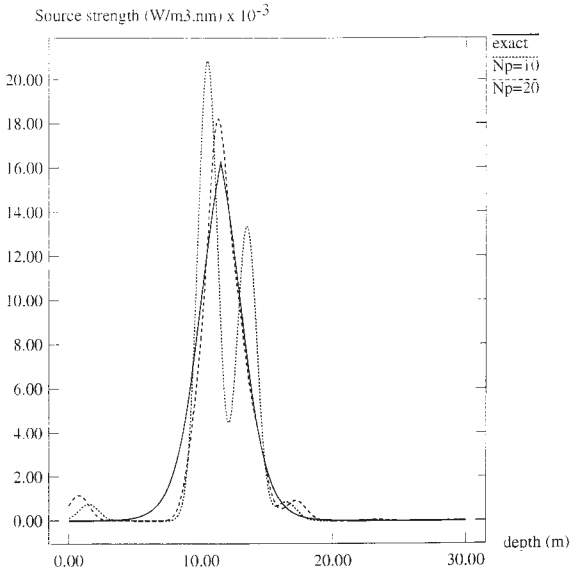

Figure 5. Influence of the number of sources in the inverse solution (case 2, 2% noise, σ = 0.75).

standard deviations in the estimation was analyzed. A significant issue to point out is that the representation of the unknown bioluminescent profiles by means of Gaussian sources make unnecessary the use of any regularization technique once these functions are inherently smooth. The extension of the present inversion technique to the estimation of inherent optical properties is currently being carried out.

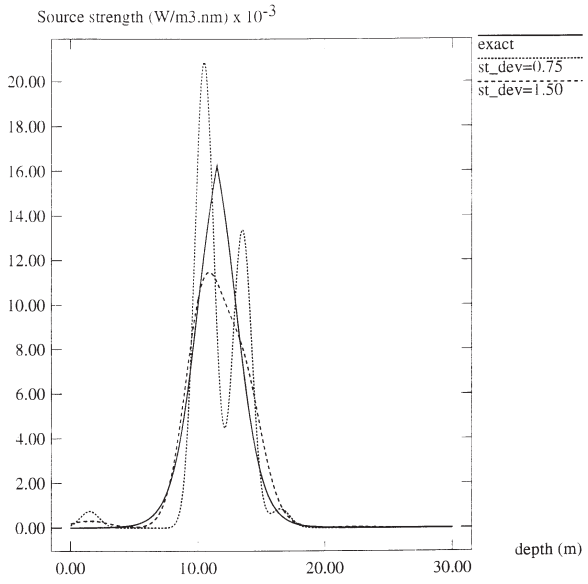

Figure 6. Influence of the standard deviations in the inverse solution (case 2, 2% noise, N_p = 10).

Acknowledgments

The authors thank FAPESP, São Paulo State Foundation for Research Support, for supporting this study through a Thematic Project grant (process 96/07200-8). C. D. Mobley acknowledges support by the Environmental Optics Program of the U.S. Office of Naval Research in developing Hydrolight.

References

1. Lesnic, D., Elliot, L., and Ingham, D. B., 1995, "An inversion method for the determination of the particle size distribution from diffusion battery measurements," *J. Aerosol Sci.* **26**(5), 797–812.

2. McCormick, N. J., 1992, "Inverse radiative transfer problems: A review," *Nuclear Sci. Eng.* **112**, 185–198.

3. Mobley, C. D., 1989, "A numerical model for the computation of radiance distributions in natural waters with wind-roughened surfaces," *Limnology and Oceanography* **34**(8), 1473–1483.

4. Mobley, C. D., 1994, *Light and Water—Radiative Transfer in Natural Waters*, Academic Press, San Diego, CA.

5. Mobley, C. D., 1995, *Hydrolight 3.0 User's Guide*, SRI International, Menlo Park, CA.

6. Mobley, C. D., Gentili, B. G., Gordon, H. R., Jin, Z., Kattawar, G. W., Morel, A., Reinersman, P., Stamnes, K., and Stavn, R. H., 1993, "Comparison of numerical models for computing underwater light fields," *Appl. Optics* **32**(36), 7484–7504.

7. NAG, 1993, *NAG Fortran Library Mark 16*, Numerical Algorithms Group, Oxford.

8. Ramos, F. M., and de Campos Velho, H. F., 1996, "Reconstruction of geoelectric conductivity distributions using a first-order minimum entropy technique," *Proceedings of the 2nd International Conference on Inverse Problems in Engineering: Theory and Practice*, Le Croisic, France.

9. Sanchez, R., Yi, H. C., and McCormick, N. J., 1992, "Bioluminescence estimation from ocean in situ irradiances," *Appl. Optics* **31**(6), 822–830.

10. Tao, Z., McCormick, N. J., and Sanchez, R., 1994, "Ocean source and optical property estimation from explicit and implicit algorithms," *Appl. Optics* **33**(15), 3265–3275.